Mineralogical Magazine, August 2016, Vol. 80(5), pp. 705–717

Usambara effect in tourmaline: optical spectroscopy and colourimetric studies

Michail N. Taran* and Ievgen V. Naumenko

Institute of Geochemistry, Mineralogy and Ore Formation, National Academy of Sciences of Ukraine, Palladin avenue 34, Kiev-142, 03680 Ukraine

[*Received 28 April 2015; Accepted 25 June 2015; Associate Editor: Ed Grew*]

ABSTRACT

The Usambara effect, i.e. a change of tourmaline colour from deep-green to dark-red with increasing path length of light, has been studied by optical absorption spectroscopy and colourimetric calculations on a sample of Tanzanian tourmaline of predominant dravite composition with 0.12 apfu Cr. For comparison a dark-green vanadium-bearing tourmaline from Tanzania (0.05 apfu V), which does not show such an effect, was also investigated. As established, the Usambara effect, by its nature, is closely related to the alexandrite effect, although in this case the colour change is not caused by change of spectral composition of the light of illumination, but by spectral positions of the spin-allowed absorption bands of Cr^{3+}, a specific ratio of light transmission in two windows of transparency, green and red, and by non-linear, exponential dependence of the light transmittance on the thickness of sample. A threshold chromium content must be exceeded for the Usambara effect to show, that is, sufficient chromium for there to be two deep and well-demarcated windows of transparency in the visible range. The overall colouration results from mixing of two additive colours coming through the windows of transparency. A dark-green chromium-bearing tourmaline from the Ural Mountains (0.40 and 0.20 apfu Cr and Fe, respectively) shows how admixtures of other chromophore ions, namely, Fe^{2+} and Fe^{3+}, can suppress the Usambara effect in tourmaline.

Keywords: tourmaline, optical spectroscopy, colour, pleochroism.

Introduction

A new and relatively little-studied characteristic of some varieties of tourmaline is the Usambara effect, named by Halvorsen and Jensen (1997) for the Usambara Mountains in northeastern Tanzania, which is the source of the chromium-bearing dravite showing this effect. The effect is manifested during illumination by intense concentrated light as an amazing change of colour from deep-green to dark-red when a critical thickness is exceeded[1]. The phenomenon is especially striking when the colour of two crystals or polished plates of such tourmaline, sufficiently thin individually to appear green, change to red when superimposed on one another. In usual diffuse daylight illumination large untreated crystals of tourmalines with the Usambara effect look black with dusk-green and reddish flashes, dependent on crystal shapes and dissipation of the light on edges and inner defects (Fig. 1). Note that the Usambara effect was recently also established on Tanzanian gem-quality chromium- and vanadium-bearing

[1]Such extreme conditions observed in the colour of tourmalines with the Usambara effect are far beyond the standards of existing colourimetric systems. Therefore, the colour coordinates calculated from optical transmission spectra of such tourmalines (e.g. XYZ coordinates of CIE system; see Liu *et al.*, 1999) correspond to achromatic black colour. It is easy to check this using the colourimetric web-calculator at http://www.easyrgb.com/index.php?X=CALC

*E-mail: m_taran@hotmail.com
DOI: 10.1180/minmag.2016.080.016

FIG. 1. Tanzanian tourmaline crystals showing the Usambara effect.

garnets of spessartine–pyrope composition (Krzemnicki, 2014) and in some types of synthetic alexandrite (Schmetzer *et al.*, 2013).

A number of publications in the gemmological literature are devoted to investigations of the Usambara effect, notably the three papers co-authored by Halvorsen. Liu *et al.* (1999) modelled transmission spectra of such a tourmaline for different thicknesses, studied changes of its colour using colourimetric calculations and arrived at the conclusion that the effect is a combination of the alexandrite effect and the influence of path length on light transmission through the crystal. Halvorsen (2006) also reported on a relationship between alexandrite and Usambara effects and considered them among other colour-change phenomena in crystals such as pleochroism, concentration effect and thermochromy.

In this paper new data on optical absorption spectroscopy and colourimetric characterization of Tanzanian tourmalines with the Usambara effect are represented.

Samples

Several large (~1.5 cm × 1.5 cm × 1.0 cm) high-quality tourmalines with the Usambara effect (Fig. 1) were bought at Kisiwani village, Tanga Province in North-Eastern Tanzania. One of the authors, N.I.V., visited the deposit near the village where the samples were taken from. At that time the place appeared to be an entirely worked-out excavation filled by clay and water. Just a few small fragments of tourmaline crystals were found at the location, good evidence that it was indeed the place where the tourmalines were taken from. A sample for investigation (tourmaline #1) was cut out as a plate parallel to the prism face of a large crystal (~2 cm × 2 cm × 4 cm), ground to a thickness of 0.40 mm and polished on both sides, suitable for measuring polarized optical absorption spectra in the range 300 to 2400 nm (~33,300 to 5560 cm^{-1}). A dark-green tourmaline crystal (tourmaline #2), which does not display the Usambara effect, was

TABLE 1. Results of microprobe determination of the tourmaline compositions (average of five measurements). Fluorine is not determined.

	Sample #				Sample #		
Oxide, wt. %	1	2	3	Elements, apfu	1	2	3
SiO_2	36.95	36.97	37.07	Si	5.94	5.97	6.03
TiO_2	0.38	0.51	0.05	Ti	0.15	0.20	0.02
Al_2O_3	29.88	28.02	30.04	Al	5.66	5.33	5.76
V_2O_3	0.05	0.42	0.05	V	0.01	0.05	0.01
Cr_2O_3	0.94	0.07	3.07	Cr	0.12	0.01	0.40
MgO	13.45	14.92	10.20	Mg	3.23	3.59	2.47
CaO	1.42	2.30	0.02	Ca	0.25	0.40	0.00
MnO	0.04	0.04	0.06	Mn	0.01	0.01	0.01
FeO	0.06	0.04	1.44	Fe	0.01	0.01	0.20
NiO	0.00	0.04	0.48	Ni	0.00	0.01	0.04
Na_2O	2.30	2.16	3.15	Na	0.72	0.68	0.99
B_2O_3*	10.8	10.8	10.7	B	3.00	3.00	3.00
H_2O*	3.72	3.72	3.69	H	4.00	4.00	4.00
Total	99.99	100.01	100.02	Total	23.1	23.26	22.93

*Calculated from stoichiometry.

https://doi.org/10.1180/minmag.2016.080.016 Published online by Cambridge University Press

bought at the same mineral market, though the exact place it was found is not known. It was ground to a thickness of 3.31 mm and polished parallel to the *c* axis suitable for measuring spectra in the same spectral range as above, ~33,300 to 5560 cm^{-1}.

Tourmaline #3 was represented by numerous well-formed thin and long prismatic (needle-like) dark-green micro-inclusions in a large quartz crystal from Zolotaya Gorka, Ural Mountains, Russia. Several fragments of these inclusions were extracted from the quartz wherein it reached the crystal surface. One inclusion 0.2 mm thick and ~0.5 mm long that was highly transparent and free from any visible imperfections was used, unpolished, for spectroscopic investigation. It was partially immersed into a droplet of glycerol upon the surface of a glass plate and, thus, served as a sample for spectroscopic measurements.

Orientations of the samples were controlled by conoscopic observation under a polarizing microscope. In all cases it does not deviate more than 5° from the true one (parallel to the *c* axis of the crystal) appropriate for measuring polarized optical absorption spectra, E||c and E⊥c.

Experimental methods

The compositions of the tourmalines were determined using a PEMMA-202M field-emission scanning electron microscope equipped with an energy-dispersive Link Systems spectrometer. Synthetic augite (STD009 standard), apatite (USNM104021) and jadeite (STD048) were used for calibration. Raw counts were corrected for matrix effects with the *ZAF* algorithm implemented by Link Systems. Five spots per sample were analysed. The results are evidence of the sample homogeneity. Fluorine was not analysed. The B_2O_3 and H_2O content were taken from stoichiometry, assuming that B = 3 atoms per formula unit (apfu) and OH = 4 apfu.

Optical absorption spectra were measured in the range 330–2500 nm (~30,000–4000 cm^{-1}) with a single-beam microspectrophotometer constructed on the basis of a SpectraPro-275 triple-grating monochromator, highly modified polarizing mineralogical microscope MIN-8 and IBM PC. An Ultrafluars 10 × served as the objective and condenser. Polarized radiation was achieved by using a Glan-Thompson-type calcite polarizer. Changeable photoelectric multiplying tubes and a cooled PbS-cell were used as photodetectors. A mechanical highly stabilized 300 Hz-chopper and lock-in amplifier were applied to improve the signal/noise ratio. The spectra were scanned with steps $\Delta\lambda$ = 0.5 nm, 1 nm, 2 nm, 5 nm and 10 nm in the range 300–350, 350–450, 450–1000, 1000–1800 nm and 1800–2500 nm, respectively. The diameter of the measuring spot was not larger than 200 μm. All spectra are normalized to 1.0 cm thickness. The resultant linear absorption coefficient was then plotted *vs*. the wavenumber.

Results and discussion

Composition

The microprobe compositions (Table 1) are evidence that all three tourmalines studied are of predominantly dravite compositions. Recalculation to crystal formula coefficients gives the following simplified results:

tourmaline #1 – $(Na_{0.72}Ca_{0.25})_{0.97}$
$(Mg_{3.23}Al_{5.66}Cr_{0.12})_{9.01}B_3Si_{5.94}O_{27}(OH)_{4.00}$;
tourmaline #2 – $(Na_{0.68}Ca_{0.40})_{1.08}$
$(Mg_{3.59}Al_{5.33}V_{0.05}Cr_{0.01})_{8.98}B_3Si_{5.97}O_{27}(OH)_{4.00}$;
tourmaline #3 – $Na_{0.99}$
$(Mg_{2.47}Al_{5.76}Cr_{0.40}Fe_{0.20}Ni_{0.06})_{8.84}$
$B_3Si_{6.03}O_{27}(OH)_{4.00}$.

As seen from Table 1, regarding chromophore ions (transition metal ions), which usually cause the colour of natural tourmalines, the Tanzanian samples #1 and #2 are essentially iron-free. The chromium content in tourmaline #1 is more than an order of magnitude higher than in #2. On the other hand, the vanadium content in the latter is nearly five times higher than in the former. Tourmaline #3 from the Ural Mountains (Russia) differs from the Tanzanian samples, #1 and #2, firstly by relatively high iron content (0.20 apfu). Additionally, the chromium content is more than three times higher than in tourmaline #1. Also it contains 0.04 apfu of nickel, whereas vanadium was not detected.

Optical absorption spectra

The polarized optical absorption spectrum of tourmaline #1 together with results of its curve-fitting analysis for two polarizations, $E\perp c$ and $E\|c$, are shown in Figs 2*a* and 2*b*, respectively. In the near-UV and visible range it consists of a high-energy absorption edge and two broad bands, ν_1 and ν_2, caused by electronic spin-allowed *dd* transitions: $^4A_{2g}\rightarrow{}^4T_{2g}$ and $^4A_{2g}\rightarrow{}^4T_{1g}$ of Cr^{3+} in

https://doi.org/10.1180/minmag.2016.080.016 Published online by Cambridge University Press

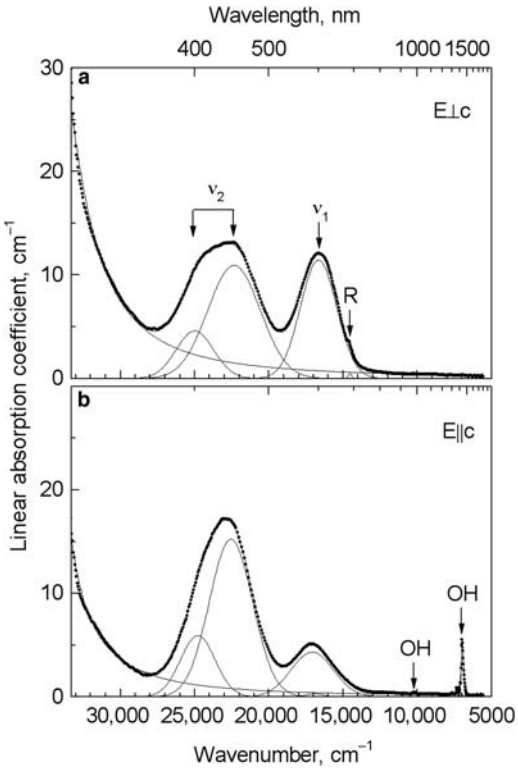

FIG. 2. Polarized optical absorption spectrum of tourmaline #1 with the Usambara effect and results of the curve-fitting analysis: (*a*) E⊥c and (*b*) E||c polarization. The dots are experimental data obtained by the single-beam procedure of registration of optical absorption spectra.

the octahedral *Y* site of the tourmaline structure. The ν_2 band is evidently split to at least two components due to the low symmetry of the position. The numerical results of the curve-fitting analysis of the spectrum of Cr^{3+} are summarized in Table 2.

The distinct *E*⊥*c*-polarized absorption peak at ~14,620 cm^{-1}, labelled in Fig. 2*a* as R, is undoubtedly caused by the electron spin-forbidden transition $^4A_{2g} \rightarrow {}^2T_{1g}$ of $^{[6]}Cr^{3+}$. Note that such an absorption feature is rather typical in the spectra of many Cr^{3+}-bearing minerals (e.g. Burns, 1993).

A spectrum, similar to that of tourmaline #1 in Fig. 2, was described recently by Bosi *et al.* (2013) in iron-bearing chromo-alumino-povondraite with 1.94 apfu of Cr^{3+}. The higher energies of the spin-allowed bands of Cr^{3+}, when compared to tourmaline #1, are most probably due to the concentration shift (e.g. Burns, 1993) caused by substitution of larger Mg^{2+} (octahedral ionic radius 0.72 Å) by smaller Cr^{3+} (0.615 Å) in the octahedral *Y* site of the structure.

A characteristic peculiarity of the spectrum in Fig. 2 is a very weak, if any (see also Fig. 3), intensity of broad absorption bands at ~14,000 cm^{-1} and 9000 cm^{-1}, which are very common in spectra of natural (e.g. Smith and Strens, 1976; Smith, 1978; Mattson and Rossman, 1987) and synthetic (Taran *et al.*, 1993) tourmalines bearing Fe^{2+} and Fe^{3+}, and which are interpreted as a split electron spin-allowed $^5T_{2g} \rightarrow {}^5E_g$ transition of Fe^{2+} involved into an exchange-couple interaction with Fe^{3+} ions occupying adjacent *Y* sites of the structure. As seen in Fig. 3, where a near-infrared part of the spectrum is shown in a larger scale, there is just a hint of a lower energy band at ~9300 cm^{-1} in E⊥c. Its low intensity, ~0.1 cm^{-1}, is consistent with the negligible iron content (Table 1). The higher energy band of the doublet, at ~14,000 cm^{-1}, cannot be seen at all as it is overlapped fully by the intense ν_1 band of Cr^{3+}.

In the E||c polarization in the range of the first OH-vibration overtone, at 6990–7650 cm^{-1}, there is a series of sharp narrow absorption lines with the strongest and relatively broad component at ~7000 cm^{-1} (Figs 2*b*, Fig. 3). In general, these lines resemble the *E*||*c*-polarized absorption lines in spectra of red Fe^{3+}-bearing dravites from Osarara in Kenya (Mattson and Rossman, 1984; Taran and Rossman, 2002) and Engusero Sambu in Tanzania (Taran *et al.*, 2015). We cannot exclude that the trivalent cations such as Fe^{3+} and Cr^{3+} were incorporated in the YO_4OH_2 octahedra of the tourmaline structure, namely, the substitution of divalent Mg^{2+} by trivalent Cr^{3+} in tourmaline #1 with the very probable substitution of at least one hydroxyl OH^- by O^{2-} in the surrounding ligands for the charge balance ($Mg^{2+} + OH^- \rightarrow Cr^{3+} + O^{2-}$), may be a cause of relatively low intensity and the characteristic configuration of the spectrum in this spectral range. Note that the second overtone of the stretching O–H vibrations is also seen in *E*||*c* polarization (Fig. 3) as a very weak asymmetric line with a maximum at ~10,220 cm^{-1}.

The polarized spectrum of tourmaline #2 together with the results of its curve-fitting analysis is shown in Fig. 4. At first glance there are some noticeable similarities between the spectra of the two tourmalines, #1 and #2 (cf. Fig. 2 and 4), both consisting of the two broad bands in the visible range symbolized as ν_1 and ν_2. However, in the two samples the bands differ significantly in intensity ratios, energies and widths of the derived curve-

https://doi.org/10.1180/minmag.2016.080.016 Published online by Cambridge University Press

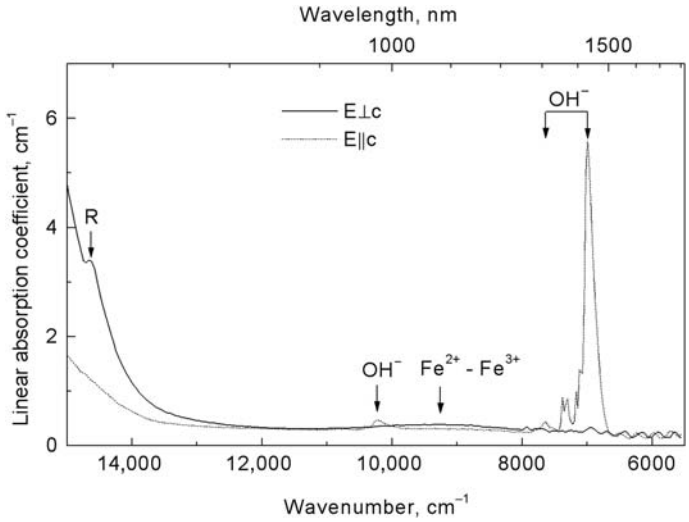

FIG. 3. The near-infrared part of the optical absorption spectrum of tourmaline #1 from 15,000 to 5500 cm^{-1}. A very weak broad E⊥c-polarized band at ~9300 cm^{-1} is caused by electron transition of the $Fe^{2+} – Fe^{3+}$ exchange-coupled pair and is evidence of a very low Fe content in the sample. The series of the weak equidistant artefacts below ~7500 cm^{-1} is most probably due to light interference in the gap between the polished surfaces of the sample and a supporting glass plate.

fitting components (Table 2). Taking into consideration much lower chromium and much higher vanadium contents in tourmaline #2 compared with tourmaline #1 (Table 1), we assume that ν_1 and ν_2 bands in the spectra in Fig. 4 are caused by electron spin-allowed transitions $^3T_{1g}$ (^3F)→$^3T_{2g}$ (^3F) and $^3T_{1g}$ (^3F) → $^3T_{1g}$ (^3P) of V^{3+} in the octahedral *Y* site of the tourmaline structure. The absence of any signs of the R-line, typical of Cr^{3+} (see above), but not V^{3+}, in the *E*⊥*c*-polarized spectrum in Fig. 4*a*, is also evidence in favour of such an interpretation.

There is very little information in the literature about the optical spectra of V-bearing tourmalines. The two most important papers are those by Schmetzer *et al.* (2007) on vanadium-bearing, gem-quality calcic aluminous dravites from Madagascar and by Ertl *et al.* (2008) on green V- and Cr-bearing olenite from a graphite deposit near Amstall, Lower Austria. Both papers describe iron-free, low-chromian V-bearing tourmalines, similar to tourmaline #2 studied here. Nevertheless, their spectra differ noticeably from the latter, especially in the energies, shapes and intensity ratios of polarized components of the ν_2 band. In particular, the broad, intense *E*⊥*c*-polarized band at 26,980 cm^{-1} (Table 2), which was not observed by Schmetzer *et al.* (2007) or Ertl *et al.* (2008), cannot be attributed to V^{3+}. Therefore, we assume that it is caused by colour centres other than V^{3+}, although at present its nature remains uncertain.

The polarized absorption spectrum of tourmaline #3 is shown in Fig. 5. The intensities of the absorption bands ν_1, ν_2 and R of Cr^{3+} in this sample are much higher than in tourmaline #1 (Fig. 2), which is consistent with the higher chromium content in the former (0.40 apfu) compared with the latter (0.12 apfu). In addition to the Cr^{3+} bands, there are two broad *E*⊥*c*-polarized absorption bands with maxima at ~13,800 and 9100 cm^{-1}, caused by electron transitions in exchange-coupled $^{[Y]}Fe^{2+}$–$^{[Y]}Fe^{3+}$ pairs (see above), whose presence is in good agreement with the high concentration of iron, 0.20 apfu, in the sample. Most probably, the intense strongly dichroic (*E*⊥*c* >> *E*||*c*) high-energy absorption edge is also caused by high Fe content. It overlaps the ν_2 band of Cr^{3+} in *E*⊥*c* polarization, so that the splitting of it is not as distinct as in iron-free tourmaline #1 (cf. Figs 2 and 5).

In E||c polarization there is a series of narrow absorption lines in the range of the first overtone of the stretching vibrations in OH groups, which differs noticeably from those in the spectra of samples #1 and #2 in Figs 2 and 4. This may be due to the relatively high Fe content in the sample #3. Also, this may be caused by influence on OH vibrations of sodium, whose content is much higher than in tourmalines #1 and #2 (Table 1).

https://doi.org/10.1180/minmag.2016.080.016 Published online by Cambridge University Press

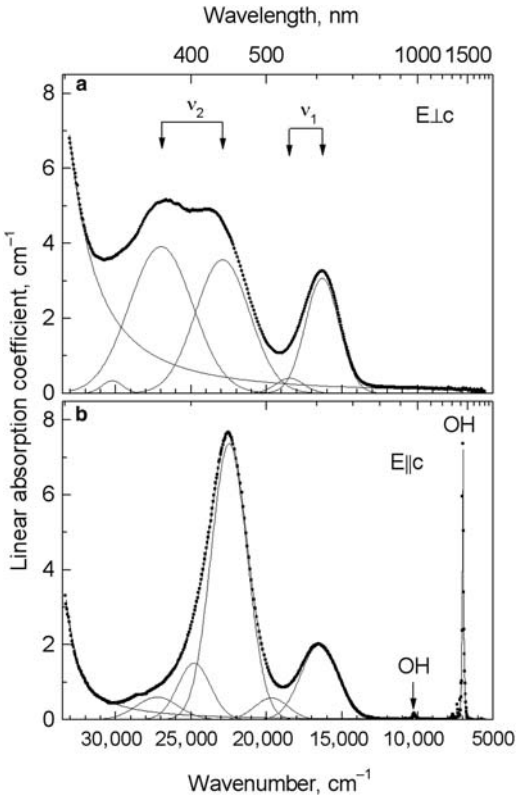

FIG. 4. The polarized optical absorption spectrum of tourmaline #2 with no Usambara effect with the results of the curve-fitting analysis: (*a*) E⊥c and (*b*) E||c-polarization. The dots are experimental data obtained by the single-beam procedure of registration of optical absorption spectra.

Colourimetric calculations

Using the Lambert–Beer law, $I = I_0 10^{-\alpha d}$, where I_0 and I are intensities of the incident- and the transmitted-light beam, respectively, α is the linear absorption coefficient and d is the distance along the path through the medium (sample thickness), and, ignoring light scattering on the surfaces and inner defects of the sample, the transmission spectra $T = f(\lambda)$, where $T = I/I_0$ and λ is wavelength, can be calculated from the polarized spectra for different sample thicknesses. For example, the results of such calculations for tourmaline #1 in $E \perp c$ polarization (Fig. 2*a*) for a thickness decreasing from 10 mm to 0.5 mm are shown in Fig. 6*a*. From them the colour coordinates λ_D, p_C and Y of the CIE 1931 XYZ colour space (e.g. Judd and Wyszecki, 1963) were calculated (see details in Table 3).

As seen from Fig. 6*a*, at thickness 10 mm in the visible range, ~380–750 nm, there is only one long-wavelength window of transparency, which causes a very saturated ($p_C = 0.98$) red colour of the sample ($\lambda_D = 620$ nm) in transmitted polarized light of the standard CIE 1931 illuminator C, imitating daylight (Judd and Wyszecki, 1963). However, the zero value of the brightness parameter, Y (Table 3), is evidence that at this standard illumination the colour of the samples is completely black. The red colour is discernible only when the sample is illuminated by intense concentrated transmitting light.

At a gradual decrease of the sample thickness, the transmittance in the long wavelength part of the spectrum increases and, additionally, at thicknesses between 5 and 2.5 mm another window of transparency in the green part of the visible range with a maximum at ~520 nm arises and gradually increases (the red and the green windows of transparency, respectively). The colour of the sample is now a mixture of two colours, red and green, the ratio of which changes with changes in sample thickness.

As seen from Fig. 2*b*, such two deep well-separated windows of transparency as in $E \perp c$ polarization, cannot be in $E \| c$ polarization, because in the latter case the intensities of the two absorption bands, ν_1 and ν_2, are essentially different and, also, because the wavelength position of the ν_1 band (Table 2) is shorter, the overlapping of the two bands, ν_1 and ν_2, is stronger than in $E \perp c$ polarization.

The chromaticity diagram xy CIE 1931 (e.g. Judd and Wyszecki, 1963) with the loci of the sample colour as a function of its thickness at two polarizations, $E \perp c$ and $E \| c$, are shown in Fig. 7. For $E \perp c$ polarization, as also seen from Table 3, with decreasing thickness from ~5.0 to 2.5 mm the colour changes from a dark-red to saturated green, and at further thinning down to 0.5 mm it remains green, retaining the dominant colour wavelength $\lambda_D \approx 535$ nm. Naturally, the saturation (purity) of the colour, p_C, decreases (the loci gradually converge at the white colour point, C, as thickness decreases from 2.5 to 0.5 mm (see also Table 2)). The values of the brightness parameter Y are evidence that the calculated colour changes from a very dense dark-red, practically black, through dark-yellow to a saturated green and then to light-green.

In E||c polarization the dominant wavelength λ_D also changes with decreasing thickness, but to a much lesser extent than in $E \perp c$: taking into consideration the brightness, Y (Table 2), it varies from a dense dark-brown, practically black, to greenish-yellow. Therefore, according to our calculations, the Usambara effect in Cr-rich tourmaline,

https://doi.org/10.1180/minmag.2016.080.016 Published online by Cambridge University Press

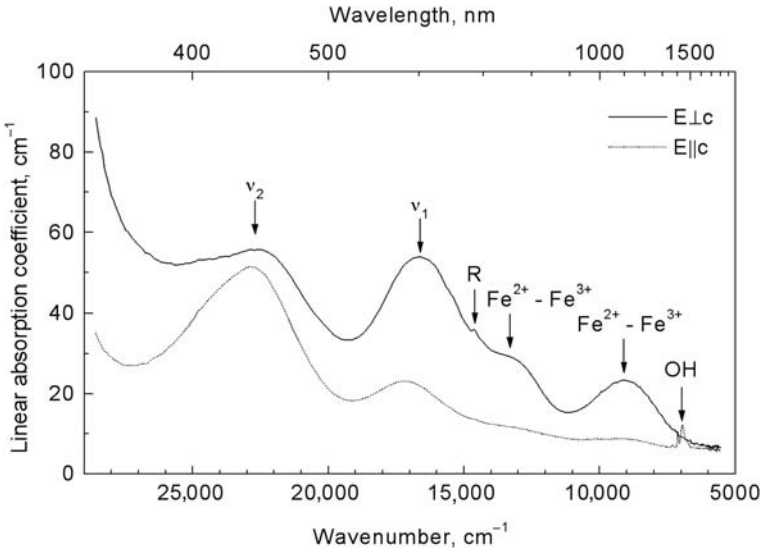

FIG. 5. The polarized optical absorption spectrum of tourmaline #3 from Zolotaya Gorka (Urals, Russia).

as defined as a contrast colour change from red to green in a certain critical range of sample thicknesses, is more prominent in $E\perp c$, than $E\|c$ polarization. At an ordinary diffuse daylight transmitting illumination this effect should be more distinct in (001) section when observed down the c axis of a crystal, as in such a case the vector of the electric field $\overline{E}$ of radiation is oriented perpendicular to the c axis, i.e. the conditions of $E\perp c$ polarization are nearly realized. Indeed, by our observations, the Usambara effect in our samples is most distinct at such conditions, i.e. at illumination and observation along the c axis.

Similar calculations for tourmaline #2, which displays no Usambara effect, is evidence, as seen from Fig. 8, of a rather different dependence of colour on sample thickness, when compared to tourmaline #1. Thus, with decreasing thickness from 10 mm to 0.5 mm, in $E\perp c$ polarization there takes place a gradual decrease of the colour saturation, p_C, (with a concomitant increase of the brightness Y) without any drastic change of the dominant colour wavelength λ_D as in tourmaline #1, or, in other words, the values of the dominant wavelength are evidence that the colour remains green. In polarization $E\|c$ it changes from dark-green, nearly black, to light greenish-yellow. Therefore, the delicate balance of optical transmission in the two windows of transparency, red and green, which is necessary for manifestation of the

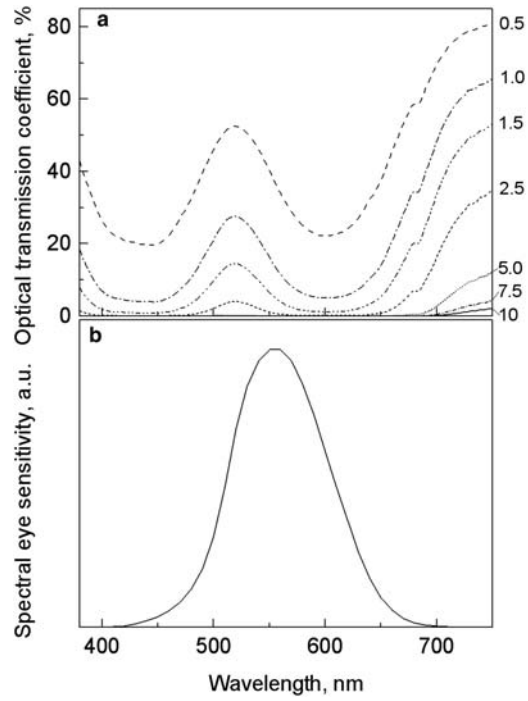

FIG. 6. (*a*) Optical transmission spectra in $E\perp c$ polarization of tourmaline #1 in the visible range, calculated for different sample thicknesses (in mm, values on the right axis); and (*b*) the curve of spectral sensitivity of the human eye in the colorimetric CIE 1931 system.

https://doi.org/10.1180/minmag.2016.080.016 Published online by Cambridge University Press

Usambara effect, does not hold in V-bearing tourmaline #2 because of the lower intensities of ν_1 and ν_2 bands and a somewhat different shape of the absorption spectrum in $E\perp c$ polarization, causing a broader 'green' window of transparency than in tourmaline #1 (cf. Figs 2 and 4).

Similarly, from $E\perp c$ and $E\|c$ polarized absorption spectra of tourmaline #3 the colourimetric characteristics were calculated for several sample thicknesses ranging from 1.5 mm to 0.2 mm. The results are evidence that in $E\perp c$ polarization the dominant colour wavelength, λ_D, depends weakly on the sample thickness (Fig. 9). With increasing thickness the colour purity, p_C, increases and the brightness Y decreases, resulting in a quick change of the sample colour from dark-green to black. It means that in contrast to tourmaline #1 (cf. Figs 7 and 9), in this sample in $E\perp c$ polarization there is no drastic change of λ_D with changes in thickness. Therefore, according to our calculations, in Cr- and Fe-bearing tourmaline #3 the Usambara effect does not appear. Note that for these two samples, #1 and #3, the dependences of λ_D on thickness in $E\|c$ polarization are also significantly different, but not as much as in polarization $E\perp c$ (cf. Figs 7 and 9). However, we believe, the change of colour in $E\|c$ polarization cannot be classified as the Usambara effect, because no drastic green-to-red colour change takes place. In this case it can be classified only as a gradual change of hue.

Halvorsen (2006) found that the Usambara effect interacted with the alexandrite effect, i.e. sensitivity of colour to the character of illumination: daylight or the tungsten-lamp light. Our tourmaline #1 with the Usambara effect, in a polished plate cut parallel to the c axis of thickness 0.4 mm (see Samples section), in unpolarized light shows no alexandrite effect. As a thick flat crystal (Fig. 1, the crystal on the right side) it becomes sensitive both to the spectral composition of the illuminating light and to

TABLE 2 Parameters of the spin-allowed absorption bands ν_1 and ν_2 in spectra of Cr^{3+}- (tourmaline #1) and V^{3+}-bearing (#2) Tanzanian tourmalines as derived by the curve-fitting procedure: α_{max} is the linear absorption coefficient (in cm^{-1}); ν is the energy of band maximum (cm^{-1}); $\nu_{½}$ is half-width (full width on half amplitude) (cm^{-1}).

Sample No.				#1	#2
Absorption band					
ν_1	Component 1	$E\perp c$	α_{max}	11.4	2.9
			ν	16,660	16,200
			$\nu_{½}$	2860	2550
		$E\|c$	α_{max}	0.32	2
			ν	16,910	16,640
			$\nu_{½}$	1340	3270
	Component 2	$E\perp c$	α_{max}	-	0.65
			ν	-	17,950
			$\nu_{½}$	-	2710
		$E\|c$	α_{max}	4.3	-
			ν	17,090	-
			$\nu_{½}$	3330	-
ν_2	Component 1	$E\perp c$	α_{max}	10.9	3.4
			ν	22,350	22,840
			$\nu_{½}$	4150	4210
		$E\|c$	α_{max}	15.3	7.5
			ν	22,560	22,570
			$\nu_{½}$	3420	3280
	Component 2	$E\perp c$	α_{max}	4.6	4.05
			ν	24,990	26,980
			$\nu_{½}$	2950	5370
		$E\|c$	α_{max}	5.9	-
			ν	24,790	-
			$\nu_{½}$	3420	-

https://doi.org/10.1180/minmag.2016.080.016 Published online by Cambridge University Press

TABLE 3 Colourimetric characteristics of tourmaline #1 calculated from the polarized optical transmission spectra for CIE 1931 illuminator C at different sample thickness (d): λ_D is the dominant wavelength; p_C is the colour saturation against the C-illuminant; and Y is the colour-brightness value.

	$E \perp c$			$E \| c$		
d, mm	λ_D, nm	p_C, r.u.*	Y, %	λ_D, nm	p_C, r.u.*	Y, %
10.0	620	0.98	0.0	597	0.95	0.0
7.5	587	0.90	0.0	581	0.93	0.3
5.0	548	0.77	0.1	571	0.91	1.5
4.0	538	0.75	0.4	569	0.90	3.3
3.0	533	0.70	1.3	568	0.89	7.2
2.5	533	0.65	2.4	568	0.87	10.9
1.5	534	0.48	9.0	568	0.81	25.3
1.0	536	0.34	18.6	568	0.71	39.3
0.5	540	0.16	41.3	569	0.47	61.9

*Relative units.

the thickness of the sample, i.e. displays an odd mixture of the alexandrite and Usambara effects. Thus, when illuminated by intense daylight or an intense tungsten lamp, it looks green or red (Fig. 10, upper and lower, respectively). However, when observed along the c axis and illuminated by intense transmitted sunlight, which is enriched with red and infrared light compared to the artificial light

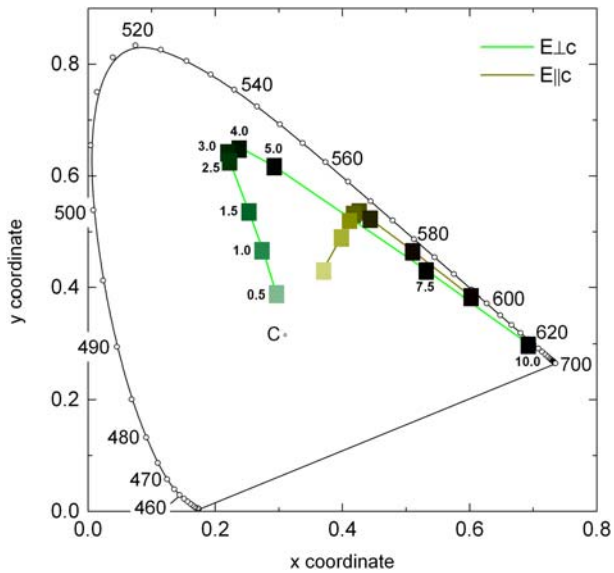

FIG. 7. Loci of tourmaline #1 in the chromaticity CIE 1931 diagram for different sample thicknesses (for clarity only numbered for $E \perp c$ polarization) in polarized light ($E \perp c$ and $E \| c$) of the standard C-illuminant. The coloured labels display the HTML colours, calculated from the spectra normalized to the different sample thicknesses for transmitting polarized light of the standard C-illuminant. The 'loop' in E⊥c polarization is evidence of the drastic change of colour from green to red known as the Usambara effect.

https://doi.org/10.1180/minmag.2016.080.016 Published online by Cambridge University Press

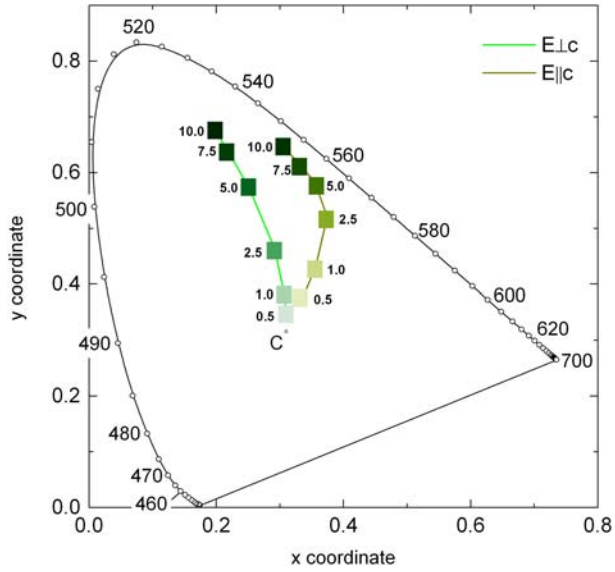

FIG. 8. As in Fig. 7, but for tourmaline #2.

of the fluorescent daylight lamp, the crystal looks red in the centre, where it is thickest due to its specific shape, and green in the rim, which is thinner. When illuminated in a similar way by a tungsten lamp, it looks entirely red.

The change of chromaticity of tourmaline #1, with change of the illumination source from C to A, as calculated from its theoretical transmittance spectrum in E⊥c polarization (see above) for a thickness of 0.5 mm, is shown by the black arrow in Fig. 11, which is a fragment of the chromaticity diagram. The labels C and A correspond to diffuse daylight and incandescent light, respectively (Judd and Wyszecki, 1963). When compared with natural alexandrite (light-grey arrow), the calculated colour change in tourmaline #1 is weaker. This may be

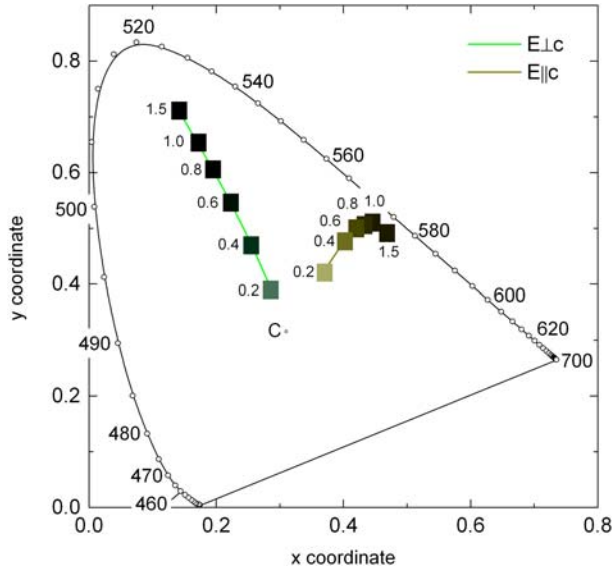

FIG. 9. As in Fig. 7, but for tourmaline #3.

https://doi.org/10.1180/minmag.2016.080.016 Published online by Cambridge University Press

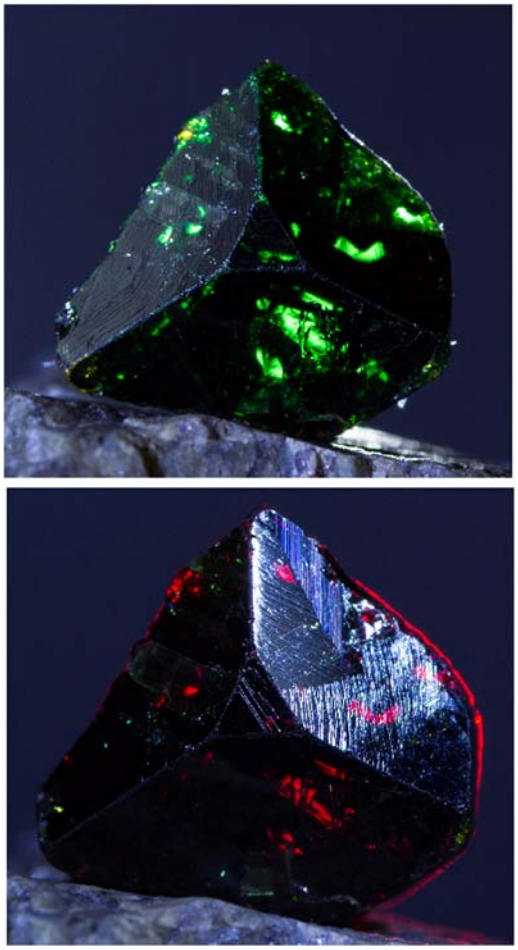

FIG. 10. A tourmaline crystal with the Usambara effect, illuminated by intense light from a daylight lamp (upper) and a tungsten lamp (lower).

caused, first of all, by the fact that the wavelengths of maxima of the spin-allowed absorption bands of Cr^{3+} in tourmaline #1 (Fig. 2), 602 nm and 438 nm, are somewhat greater than the critical values of 565–595 nm and 410–420 nm, respectively, at which Cr-bearing crystals display a colour change from green to red with a change of illumination from daylight to tungsten-lamp light, i.e. the alexandrite effect (e.g. Farrell and Newnham, 1965). In tourmaline #2 such a colour change, as seen from Fig. 11 (the grey arrow), is even weaker than in #1, because the spectral positions of ν_1 and ν_2 bands in its spectrum deviate even more from the critical values.

It is clear that for the distinct manifestation of the Usambara effect, there should be two deep and well demarcated windows of transparency in the visible range, such that the resulting colouration is formed by mixing two colours (the mixture of two light flows coming through the two windows of transparency), which are additive colours[2] with respect to each other. When two additive colours are mixed a human eye is able to perceive the resultant colouration as strongly dependent on the spectral composition of the illuminating light (the alexandrite effect) or on sample thickness (the Usambara effect). When two colours that are not additive are mixed, blue and green or green and yellow, for instance, the colour change is perceived mainly just as a change of hue.

For the appearance of the Usambara effect in tourmaline it is necessary that the 'red' window of transparency in the optical absorption spectra be deeper than the 'green' one. As the transmittance, $T = I/I_0 = 10^{-\alpha d}$, depends exponentially on sample thickness d, the integral transmittance in the 'green' window will increase faster than in the 'red' one with decreasing thickness (Fig. 6*a*). Given that the spectral sensitivity of a human eye has a maximum in the green range at ~555 nm (Fig. 6*b*), the ratio of intensities of the light passed through the 'green' and 'red' windows of transparency will change at a certain thickness of the sample, so that the visual psycho-physical perception of the colour changes from predominantly red to predominantly green. In this respect, the Usambara effect may be regarded as a specific realization of the alexandrite effect, not because of a change of the nature of the incident light, but because of the non-linear (exponential) dependence of optical transmission upon sample thickness.

The Usambara effect in tourmaline would not appear when the specific and subtle balance between intensity of light, passed through the 'green' and 'red' windows of transparency, is disturbed by a sufficiently strong change in window shape. This is shown clearly in the spectrum of tourmaline #2, in which the 'green' window in $E \perp c$ polarization is somewhat broader than in tourmaline #1.

[2]Additive (or complementary) colours are pairs of colours (e.g. green and red or blue and orange) that upon mixing give the neutral white colour (e.g. Judd and Wyszecki, 1963).

https://doi.org/10.1180/minmag.2016.080.016 Published online by Cambridge University Press

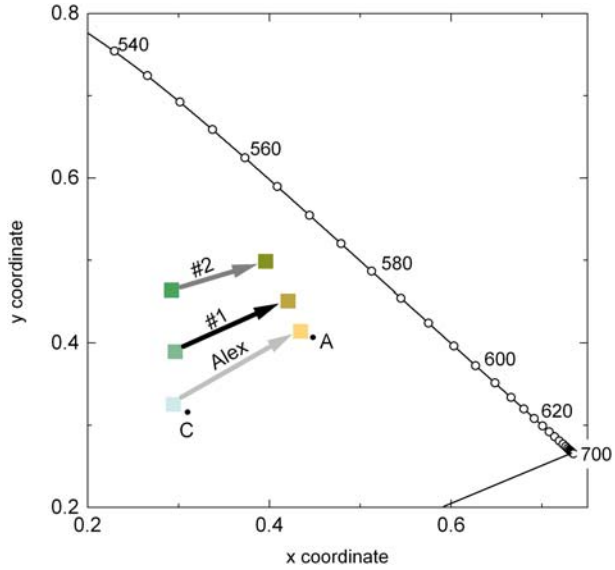

FIG. 11. A fragment of the chromaticity diagram, wherein the black arrow shows the change of chromaticity of tourmaline #1, sample thickness 0.5 mm in $E \perp c$ polarization, with change of the illuminant light source from C (daylight lamp) to A (tungsten lamp). For comparison the change of colour of tourmaline #2 ($E \perp c$, thickness 2.5 mm) is shown by the grey and that of natural alexandrite from Brazil ($E \| b$, 0.5 mm) by the light-grey arrows. The coloured labels display the HTML colours, calculated for transmitting polarized light of the standard illuminants C (left) and A (right).

It is quite obvious, that the specific ratio of optical transmittance in the two windows of transparency, 'green' and 'red', and thus the appearance of the Usambara effect in Cr^{3+}-bearing tourmalines, may be disturbed by other chromophore ions in the structure. Tourmaline #3 from the Ural Mountains can serve as a characteristic example of the destructive influence of iron on the Usambara effect. As seen from Fig. 5, because the strong high-energy edge of absorption, caused, as stated above, mainly by Fe^{3+}, and of the Fe^{2+}-Fe^{3+} exchange-coupled pair band at 9100 cm^{-1}, whose high-energy tail covers the red part of the visible range, the 'green' and 'red' windows of transparency in $E \perp c$ polarization are of nearly equal depth. This leads to violation of the specific and subtle balance of light flows transmitted through the two windows, 'red' and 'green', and, according to the colourimetric calculations (Fig. 9), to a lack of any Usambara effect in the sample studied.

Acknowledgements

We thank O.V. Andreev (Kiev) for microprobe analyses of the tourmalines studied. We are also thank two anonymous reviewers for their helpful comments, which significantly improved the paper. Especially, we are grateful to the Editorial Board Member, Ed Grew for very helpful and constructive comments and suggestions that improved the English style of the manuscript.

References

Bosi, F., Skogby, H., Hålenius, U. and Reznitskii, L. (2013) Crystallographic and spectroscopic characterization of Fe-bearing chromo-alumino-povondraite and its relations with oxy-chromium-dravite and oxy-dravite. *American Mineralogist*, **98**, 1557–1564.

Burns, R.G. (1993) *Mineralogical Application of Crystal Field Theory.* Cambridge University Press, Cambridge, UK, 550 pp.

Ertl, A., Rossman, G.R., Hughes, J.M., Chi, Ma and Brandstatter, F. (2008) V^{3+}-bearing, Mg-rich, strongly disordered olenite from a graphite deposit near Amstall, Lower Austria: A structural, chemical and spectroscopic investigation. *Neues Jahrbuch für Mineralogie – Abhandlungen*, **184/3**, 243–253.

Farrell, E.F. and Newnham, R.E. (1965) Crystal-field spectra of chrysoberyl, alexandrite, peridot, and sinhalite. *American Mineralogist*, **50**, 1972–1981.

Halvorsen, A. (2006) The Usambara effect and its interaction with other colour change phenomena. *The Journal of Gemmology*, **30**, 1–21.

https://doi.org/10.1180/minmag.2016.080.016 Published online by Cambridge University Press

Halvorsen, A. and Jensen, B.B. (1997) A new colour-change effect. *The Journal of Gemmology*, **25**, 325–330.

Judd, D.B. and Wyszecki, G. (1963) *Color in Business, Science, and Industry.* Wiley, 500 pp.

Krzemnicki, M.S. (2014) Exceptional colour change garnets showing the Usambara effect. *Facette*, **12**, 16–17.

Liu, Y., Shigley, J.E. and Halvorsen, A. (1999) Colour hue change of a gem tourmaline from Umba Valley, Tanzania. *The Journal of Gemmology*, **26**, 386–396.

Mattson, S.M. and Rossman, G.R. (1984) Ferric iron in tourmaline. *Physics and Chemistry of Minerals*, **14**, 225–234.

Mattson, S.M. and Rossman, G.R. (1987) Fe^{2+}-Fe^{3+} interactions in tourmaline. *Physics and Chemistry of Minerals*, **14**, 163–171.

Schmetzer, K., Bernhardt, H.-J., Dunaigre, C. and Krzemnicki, M.S. (2007) Vanadium-bearing gem-quality tourmalines from Madagascar. *The Journal of Gemmology*, **30**, 413–433.

Schmetzer, K., Bernhardt, H.-J., Balmer, W.A. and Hainschwang, T. (2013) Synthetic alexandrites grown by the HOC method in Russia: internal features related to the growth technique and colorimetric investigation. *The Journal of Gemmology*, **33**, 113–130.

Smith, G. (1978) A reassessment of the role of iron in the 5,000–30,000 cm^{-1} region of the electronic absorption spectra of tourmaline. *Physics and Chemistry of Minerals*, **3**, 343–373.

Smith, G. and Strens, R.G.J. (1976) Intervalence transfer absorption in some silicate, oxide and phosphate minerals. Pp. 583–612 in: *The Physics of Minerals and Rocks* (R.G.J. Strens, editor). Wiley, New York.

Taran, M.N. and Rossman, G.R. (2002) High-temperature, high-pressure optical spectroscopic study of ferric-iron-bearing tourmaline. *American Mineralogist*, **87**, 1148–1153.

Taran, M.N., Lebedev, A.S. and Platonov, A.N. (1993) Optical absorption spectroscopy of synthetic tourmalines. *Physics and Chemistry of Minerals*, **20**, 209–220.

Taran, M.N., Dyar, M.D., Naumenko, I.V. and Vyshnevsky, O.A. (2015) Spectroscopy of red dravite from Northern Tanzania. *Physics and Chemistry of Minerals*, **42**, 559–568.

https://doi.org/10.1180/minmag.2016.080.016 Published online by Cambridge University Press